Quaternary Research 86 (2016) 95–109

Contents lists available at ScienceDirect

Quaternary Research

journal homepage: http://www.journals.elsevier.com/quaternary-research

Climatic interpretation of loess-paleosol sequences at Mobarakabad and Aghband, Northern Iran

Amin Ghafarpour [a], Farhad Khormali [a, *], William Balsam [b], Alireza Karimi [c], Shamsollah Ayoubi [d]

[a] Department of Soil Science, Gorgan University of Agricultural Sciences and Natural Resources, Gorgan, Iran
[b] Department of Earth Sciences, Dartmouth College, Hanover, NH 03755, USA
[c] Department of Soil Sciences, Ferdowsi University of Mashhad, Mashhad, Iran
[d] Department of Soil Science, College of Agriculture, Isfahan University of Technology, Isfahan, Iran, 84156-83111

ARTICLE INFO

Article history:
Received 4 May 2015
Available online 24 June 2016

Keywords:
Loess
Paleosol
Magnetic susceptibility
Micromorphology
Quaternary
Northern Iran

ABSTRACT

Loess accumulation and paleosol formation are important Quaternary geoarchives in northern Iran. Two loess-paleosol sequences at Mobarakabad and Aghband were examined using soil morphology and micromorphology, mineralogy, magnetic susceptibility (MS), free Fe oxides and calcium carbonate equivalent. The loess-paleosol sequences provide a record of changes in paleo-rainfall in the northern Iran. Micromorphological and MS differences between the loess and paleosols in the sections reflect changes in climate. The different behaviors of magnetic susceptibility between Aghband and Mobarakabad loess are mainly produced by their different pedogenic environments, topography and climatic conditions. As a result, the MS at the Mobarakabad section is much higher than at Aghband. Paleoecological reconstructions coupled with magnetic depletion in paleosols at Mobarakabad suggest a wetter climate dominating during the formation of the paleosols.

Introduction

Loess deposits are well-recognized as an archive of information on Quaternary climate change and atmospheric circulation (Muhs, 2007). In mid-to high-latitude regions, an important paleoclimate record is preserved in loess modified by pedogenic processes (Catt, 1991; Begét, 2001). Loess in the mid-latitude of Eurasia provides an excellent sedimentary archive for understanding past climate and environment changes in the continental interior with important implications for aridification, dust sources, past atmospheric circulation, and past global climate change (Dodonov, 1991; Ding et al., 2002; Fang et al., 2002; Machalett et al., 2008; Song et al., 2010a). Northern Iran is a key area that connects the European and Asian loess zones. Investigations of loess-paleosol sequences from this region are important, partly due to the special location and their thickness of up to 30 m on the foothills of the Alborz Mountains and about 60 m in the Northern Iranian Loess Plateau (Lauer et al., 2015). The loess potentially records paleoenvironmental change in Iran over multiple glacial cycles, and helps to assess the extent to which key features of loess stratigraphy can be traced along the loess belt that crosses Eurasia, from Eastern Europe through Central Asia to China.

The spatial and temporal signature of loess deposits in Northern Iran is less known than loess-paleosol sequences from the Chinese Loess Plateau (e.g. Liu and Ding, 1998; Ding et al., 2002; Chen et al., 2006; Song et al., 2013) and Central Asian loess (e.g. Dodonov and Baigusina, 1995; Ding et al., 2002; Dodonov et al., 2002; Song et al., 2010a; Yang et al., 2014). Previous analyses of loess paleosol sequences in Northern Iran mainly focused on dating of deposits (Frechen et al., 2009; Lauer et al., 2015) with little emphasis on the micromorphological features to aid in understanding associated pedogenesis (Kehl et al., 2005, 2010; Khormali and Kehl, 2011; Wang et al., 2016). Recently, the loess deposits near Gorgan have been investigated in more detail (Vlaminck et al., 2015).

This study investigates two loess-paleosol sequences at Mobarakabad and Aghband in northern Iran, using macro- and micro-scale analyses. We attempt (1) to analyze the loess and paleosols soil morphology and micromorphology to estimate the degree of soil formation and explore paleoecological changes, (2) to assess the

* Corresponding author. Hezar Peach Blvd. (Pardis), Dept. of Soil Sciences, Gorgan University of Agricultural Sciences and Natural Resources, Gorgan, Iran.
E-mail addresses: Khormali@yahoo.com, fkhormali@gau.ac.ir (F. Khormali).

http://dx.doi.org/10.1016/j.yqres.2016.05.004
0033-5894/

mechanisms by which the magnetic susceptibility (MS) is enhanced in comparison to the magnetic properties of loess deposits in Romania (Constantin et al., 2014), the northern Black Sea coastal area (Dodonov et al., 2006), Siberia (Liu et al., 2008), Tajikistan (Ding et al., 2002), Ili Basin (Song et al., 2010a) and China (Song et al., 2010a); and (3) to propose a pedostratigraphical scheme for the studied sections and compare them with previously published loess-paleosol sequences at Neka, Now Deh, Aghband (Frechen et al., 2009) and Toshan (Vlaminck et al., 2015) in Northern Iran.

Location and setting

The study sites are located in Golestan province, Northern Iran (Fig. 1). The present climate in this loess region of northern Iran is characterized by hot, dry summers and mild, wet winters. Currently, in northern Iran the time of the highest wind velocity and lowest rainfall is during the early summer, especially during mid or late June. During this time it is likely that deflated eolian dust is carried by westerly air streams to the east and during the wet winter season, dust storms decrease or disappear with the increase of precipitation.

The section at Mobarakabad (37° 09′ 32″ N, 55° 18′ 14″ E), is located on the northernmost ridge of Alborz Mountains, 310 m above sea level. The total thickness of the section is about 17 m and it contains five paleosols (Fig. 2). The natural vegetation on the section is Hyrcanian forest, dominated by temperate broad-leaved deciduous trees. At present, the mean annual precipitation (MAP) and temperature (MAT) at Mobarakabad are about 670 mm and 15°C respectively. The other section is at Aghband and is located in the area between the Gorganrud and Atrek rivers on the Iranian loess plateau, 150 m above sea level. At present, MAP and MAT at Aghband are about 300 mm and 18°C respectively and the natural vegetation on the section is grassland. At Aghband, two profiles are located ~200 m away from each other were studied (Fig. 3). The main profile (37° 37′ 10″ N, 55° 09′ 42″ E) is located along a steeply inclined eastward facing slope of a loess hill. The thickness of loess deposits at this site is about 44 m and contains one paleosol (Fig. 3A). The other profile is the AG 2 paleosol (Fig. 3B) (37° 37′ 18″ N, 55° 09′ 39″ E). In this study samples were collected for MS measurements from the AG 2 paleosol, while the chemical and mineralogic analyses are presented in Khormali and Kehl (2011) and the chronological results (correlating with marine isotope stage (MIS) 5e) were published by Frechen et al. (2009).

Material and methods

Chemical and mineralogical analyses of loess and paleosols

A total of 276 samples were prepared for magnetic susceptibility (MS) measurements and chemical analyses. One hundred and

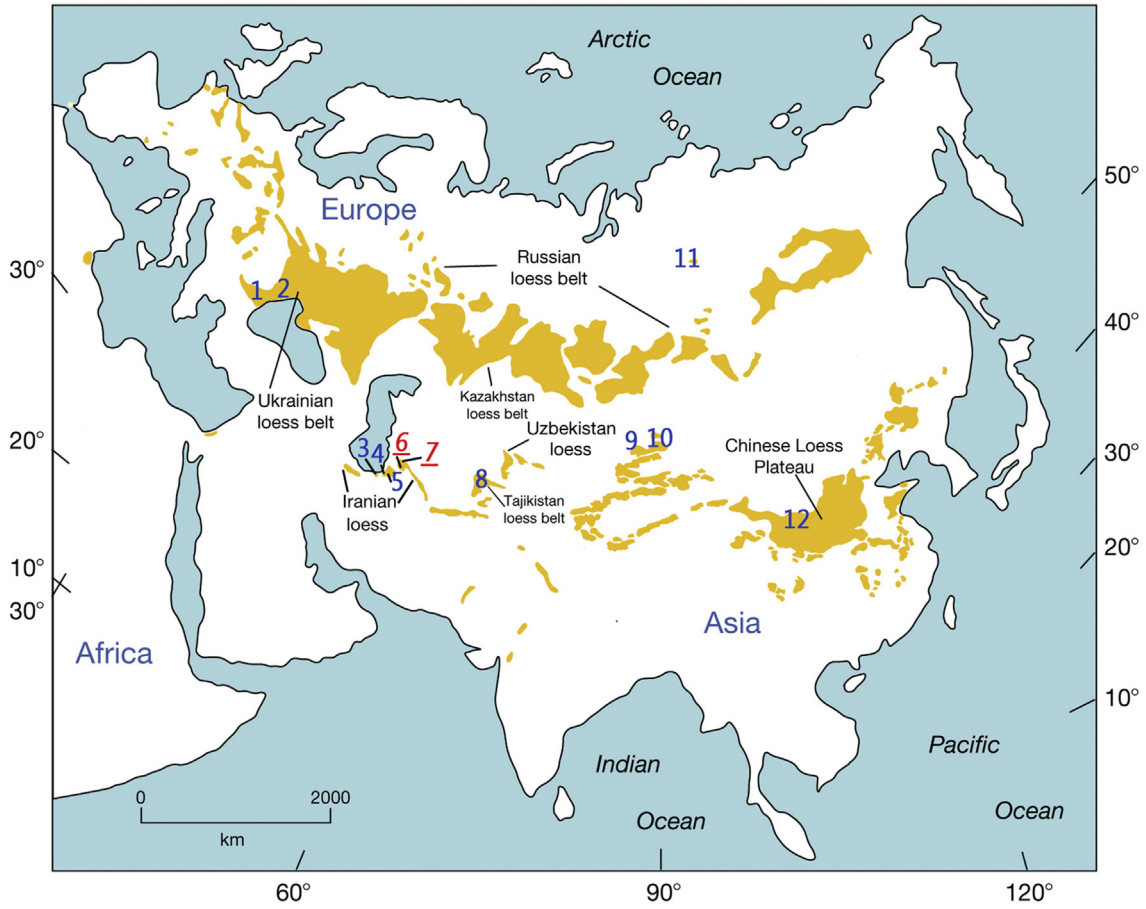

Figure 1. Map showing the distribution of loess in Eurasia (modified from Muhs, 2007) and the approximate location of studied sections and previously studied sections used in this paper. Numbers (in blue in color illustration) are based on previously published research (see Table 4 and Fig. 7 for details); underlined numbers in italics (and red in color illustration) are first reported in this paper (see Figs. 2 and 3A and Table 4 for details). The numbers correspond to the sections listed by location in Table 4 and Fig. 7. They are 1) Costineşti, 2) northern Black Sea coastal area, 3) Neka, 4) Toshan, 5) Now Deh, 6) Mobarakabad, 7) Aghband, 8) Chashmanigar, 9) Zhaosu, 10) Talede, 11) Kurtak, 12) Chaona. (For interpretation of the references to color in this figure legend, the reader is referred to the web version of this article.)

https://doi.org/10.1016/j.yqres.2016.05.004 Published online by Cambridge University Press

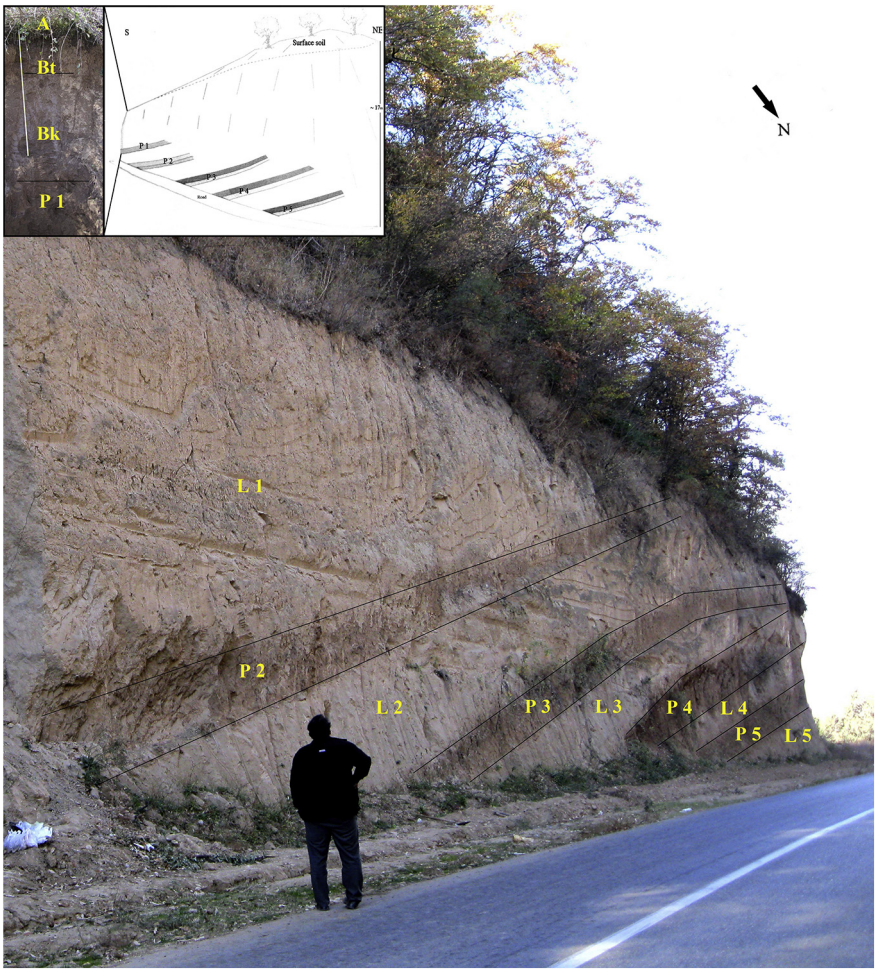

Figure 2. Photo overview of the Mobarakabad section including schematic presentation of the loess-palosols. In the section the pedocomplex sequence splits into five different paleosols that are intercalated in the loess with anticlinal shapes. Since there is no indication of modern tectonic activity in the area (Kehl et al., 2005) it is more likely that the anticlinal shape of the loess-paleosol sequence results from mantling a pre-existing land surface.

seventy one samples were collected at the Mobarakabad section at 10 cm intervals. At Aghband, 82 samples of the loess were collected at 50 cm intervals and 23 samples from the AG 2 paleosol were collected at 10 cm intervals.

Free Fe oxides (Fe_d) of the samples were determined by the citrate-bicarbonate-dithionite (CBD) method (Mehra and Jackson, 1960). Alkaline-earth carbonate was measured by acid neutralization and expressed as calcium carbonate equivalent, CCE (Salinity Laboratory Staff, 1954). X-ray diffractometry (XRD) analyses were performed on representative samples from both sections. Chemical cementing agents (carbonate, organic matter and free iron oxides) were removed and clay fractions were separated according to Mehra and Jackson (1960), Kittrick and Hope (1963) and Jackson (1975). Iron-free samples were centrifuged at 670 rpm for 5.4 min to separate total clay (<2 μm; Kittrick and Hope, 1963). The total clay fractions were analyzed mineralogically by X-ray diffractometry (Jackson, 1975). The same concentration of clay suspensions was used for all samples to yield comparisons between relative peak intensities. The (001) reflections were obtained following Mg-saturation, ethylene glycol solvation and K-saturation. The K-saturated samples were studied both after drying and after being heated at 550°C for 4 h. To identify kaolinite in the presence of tri-octahedral chlorite, samples were also treated with 1 N HCl at 80°C overnight. Clay minerals were estimated semi-quantitatively from the relative first order X-ray peak areas of glycol-treated samples (Johns et al., 1954).

Magnetic susceptibility measurements

Magnetic susceptibility of the samples was measured at low (0.47 kHz) (χ_{lf}) and high (4.7 kHz) (χ_{hf}) frequency using a Bartington magnetic susceptibility meter with MS2B dual frequency sensor. χ_{fd}%, which reflects the concentration of superparamagnetic grains in soils (Dearing et al., 1996), was calculated as $(\chi_{lf} - \chi_{hf})/\chi_{lf} \times 100\%$.

Micromorphological analysis

In Mobarakabad, undisturbed blocks were collected from each horizon of the surface soil and the B horizons of paleosols, and representative samples from loess horizons. In Aghband, the undisturbed blocks were collected from the A and C horizons of the surface soil, the Bwy horizon of the paleosol, and the loess deposits. Representative thin sections of about 60 and 30 cm^2 were prepared from air-dried, undisturbed clods using standard techniques (Murphy, 1986). Carbonate was removed from some thin sections by placing them in a 1 N HCl solution for 3 min before mounting a cover slip (Wilding and Drees, 1988). Micromorphological descriptions were made according to Bullock et al. (1985) and Stoops (2003) while the interpretation of micromorphological features followed criteria of Stoops et al. (2010). The micromorphological index of soil evolution in highly calcareous arid to semiarid conditions (MISECA) suggested by Khormali et al. (2003) was

https://doi.org/10.1016/j.yqres.2016.05.004 Published online by Cambridge University Press

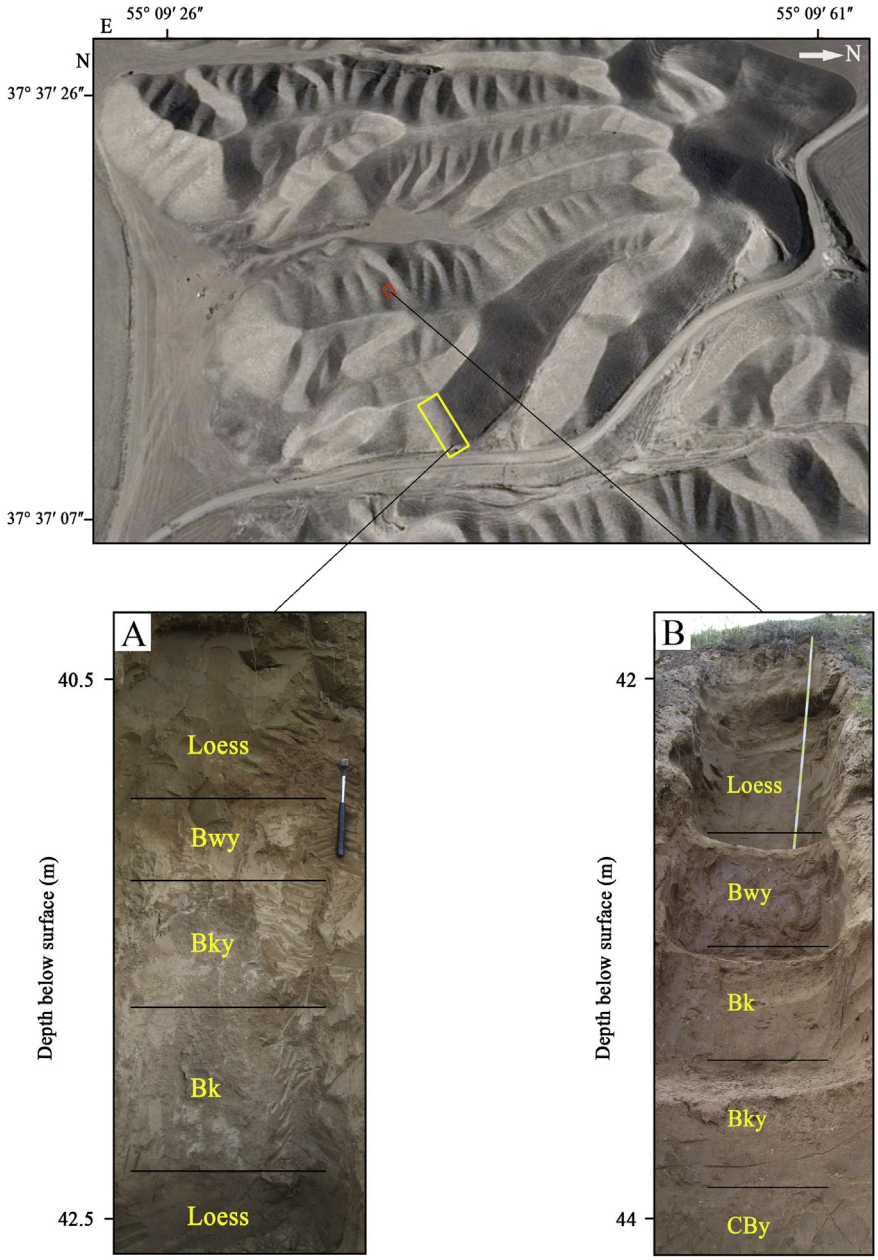

Figure 3. Picture showing the hilly landscape of the Iranian loess plateau at Aghband. The yellow and red rectangles represent the position of the main loess-paleosol section and AG 2 respectively. The paleosol horizons at the Aghband section (A); AG 2 (B). (For interpretation of the references to color in this figure legend, the reader is referred to the web version of this article.)

calculated to estimate the degree of soil development. This index includes the micro-structure, b-fabric, clay coating, decalcified zone, Fe/Mn hydroxide and alteration degree of mineral grains. With increasing degree of soil development, the MISECA values range from 0 to 24 (Khormali et al., 2003).

Results

Profile descriptions

The profile from Mobarakabad consists of a surface soil and five loess-paleosol sequences (Fig. 2), all of which overlie Jurassic-age gray massive cherty limestone bedrock. The surface soil is a Calcic Argixerolls based upon standard USDA-NRCS classifications (Soil Survey Staff, 2014) with a 1.65 m thick, A-Bt (Fig. 4A) -Bk-CBk profile. The paleosol and loess sequences are ordered from top (P 1 and L 1) to bottom (P 5 and L 5) respectively (Fig. 2 and Table 1). Paleosol 1 (P 1) is a brown Bk horizon (1.65–2.45 m) with pedogenic carbonate filaments below the surface soil. Loess 1 (L 1) is a yellowish brown horizon (2.45–4.95 m) with a coherent structure and primary $CaCO_3$ and scattered mollusc shells. It gradually merges into a CBk horizon (4.95–5.95 m). The CBk shows signs of weak browning and partially fine subangular blocky structure (Table 1). Paleosol 2 (P 2) is a brown Bt horizon (Fig. 4B) (5.95–7.15 m) with a subangular blocky structure while the voids are entirely filled with secondary carbonate precipitates. Loess 2 (L 2) extending from 7.15 to 8.65 m and consists of a yellowish brown Ck horizon and a slightly browner CBk horizon, bearing small

https://doi.org/10.1016/j.yqres.2016.05.004 Published online by Cambridge University Press

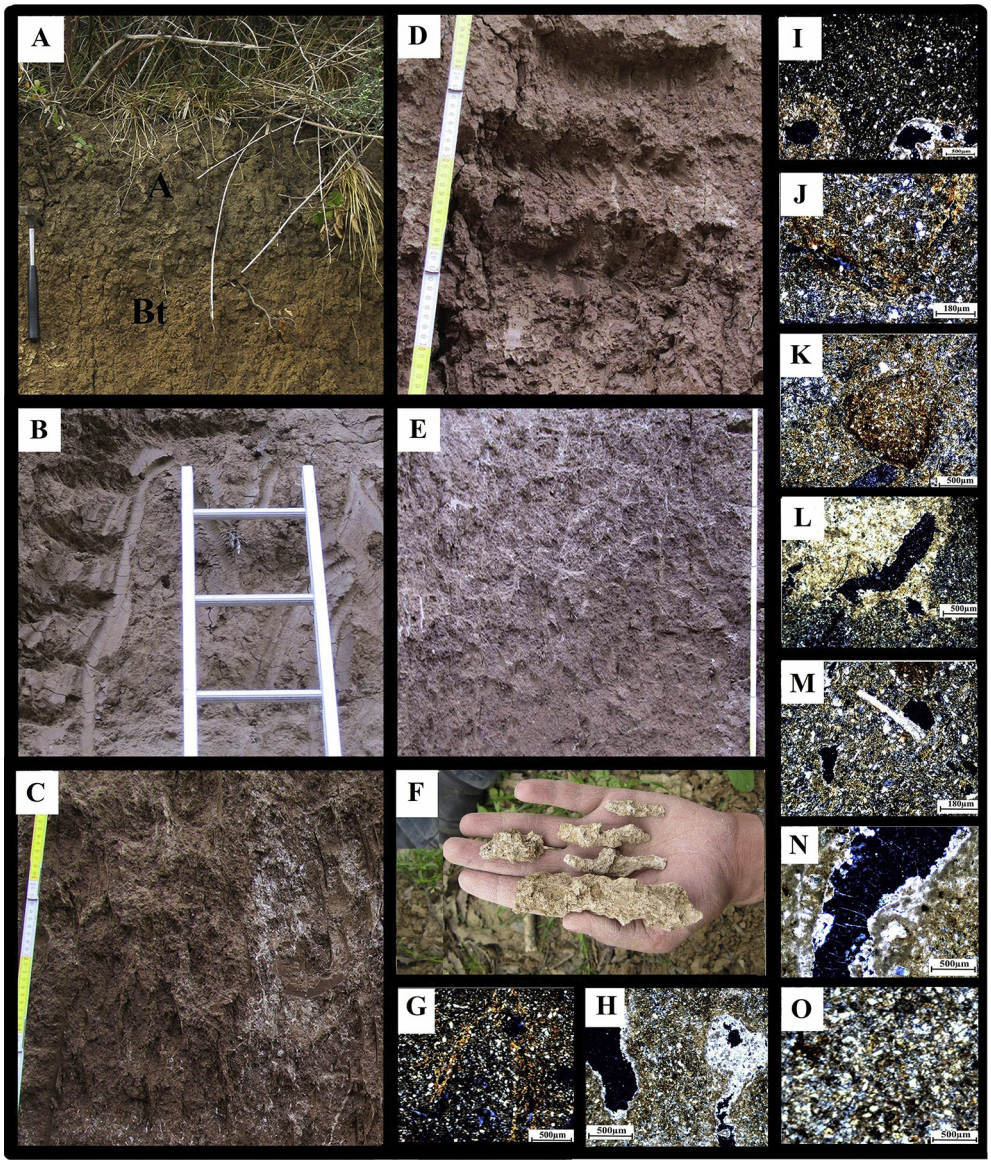

Figure 4. Outcrop and photomicrograph images of the profile at Mobarakabad wich horizon features described in Table 1. (A) A and Bt horizons of surface soil. (B) Typical Bk horizon from P 2. (C) Btk horizon from P 3. (D) Slickensides and peds from Bt horizon in P 4. (E) Btk horizon from P 5. (F) Carbonate concretions (loess dolls) observed in L 5. (G–O) Photomicrographs of the represented Loess and Paleosols along Mobarakabad and Aghband sections, all images in cross-polarized light (XPL). (G) Speckled b-fabric and clay coating within surface soil (Bt). (H) Calcite depletion and pore infillings within P 1 (Bk). (I) Calcite depletion and calcite coating around pores within P 2 (Bk). (J) Clay coating and Fe–Mn coating within P 3 (Bt). (K) Fe–Mn hydroxide nodules within P 4 (Bt). (L) Hypocoating of carbonate within P 5 (Btk). (M) Shell fragments within L 3. (N) Parallel oriented needle-fiber calcite forming in pore within CBk horizon of L 1. (O) Crystallitic b-fabric within loess at Aghband section.

subangular aggregates within a partially decalcified and coherent matrix. Paleosol 3 (P 3) is a reddish brown (Fig. 4C) from 8.65 to 9.75 m. Clay films were observed on the faces of peds and the aggregate surfaces are mottled by Fe–Mn hydroxides. Loess 3 (L 3) is a CBk horizon (9.75–11.05 m), as it shows partial decalcification, calcite coating and small Mn–Fe mottles dispersed within the stratum point to incipient soil formation. Paleosol 4 (P 4) (11.05–12.95 m), is a strongly developed dark reddish brown Bt horizon with shiny surface (Fig. 4D), Fe–Mn nodules and high calcite depletion. Loess 4 (L 4) is about 1 m (12.95–13.95 m) thick, yellowish brown and has coherent structure (Table 1). Paleosol 5 (P 5) is 1.2 m thick (13.95–15.15 m), reddish brown (Fig. 4E), thick clay skins and large Fe–Mn concretions. Loess 5 (L 5) is a yellowish brown Ck horizon 1.85 m thick (15.15–17 m) with calcite nodules and large loess dolls (Fig. 4F). From 15.45 to 16.05 m a CBk horizon is intersected in the L 5, showing a coherent to subangular blocky structure and a slightly browner color indicating a weak pedogenic imprint (Table 1).

In Aghband, the surface soil is a Typic xerorthents (Soil Survey Staff, 2014). Loess deposits about 44 m thick cover a brown paleosol (40.5–42.5 m) including brown to slightly red Bwy, brown Bky and Bk horizons (Fig. 3A and Table 1). AG 2 is a well-developed paleosol with a 2.5 m thick with Bwy, Bk, Bky and CBy horizons (Fig. 3B).

Micromorphology

Loess and paleosol field and thin section descriptions for the sections are summarized in Table 1. The main micromorphological properties and MISECA of the B horizons are shown in Table 2. At

https://doi.org/10.1016/j.yqres.2016.05.004 Published online by Cambridge University Press

Table 1
Loess and paleosol field and thin section descriptions along the sections.

Stratigraphy	Depth (m)	Description
Mobarakabad	~17	
Surface soil	0–1.65	A: 0–30 cm; dark (10 YR 3/2), organic rich, silty clay, crumb microstructure, mollic epi pedon, root traces and worm channels, excrement, speckled b-fabric, calcite depletion. Bt: 30–70 cm; reddish (7.5 YR 4/3), silty clay, angular blocky microstructure, channels and chambers, excrement, speckled b-fabric, calcite depletion, clay coating. Bk: 70–165 cm; brown (10 YR 5/3), crystallitic partially speckled b-fabric, subangular blocky microstructure, calcite nodules, calcite coating.
P 1	1.65–2.45	Bk: 165–245 cm; brown (10 YR 5/4), crystallitic partially speckled b-fabric, subangular blocky microstructure, calcite nodules, calcite coating
L 1	2.45–5.95	Ck: 245–495 cm; yellowish brown (10 YR 6/4), silt loam, uniform, massive microstructure, crystallitic b-fabric, calcite nodules, calcite coating, without clay domains. CBk: 495–595 cm; yellowish brown (10 YR 4/4), silt loam, weakly developed angular blocky microstructure, crystallitic and partially speckled b-fabric, needle-shaped calcite, calcite nodules, calcite coating, very few Fe–Mn coating, very few clay domain.
P 2	5.95–7.15	Bk: 595–715 cm; brown (7.5 YR 5/4), angular blocky microstructure, speckled b-fabric, calcite depletion, Fe–Mn coating, few clay skins.
L 2	7.15–8.65	Ck: 715–805 cm; yellowish brown (10 YR 6/4), silt loam, massive microstructure, crystallitic and partially speckled b-fabric, calcite nodules, calcite coating, without clay domains. CBk: 805–865 cm; yellowish brown (10 YR 4/4), silt loam, weakly developed angular blocky microstructure, crystallitic and partially speckled b-fabric, needle-shaped calcite, calcite nodules, calcite coating, very few Fe–Mn coating, few clay domain
P 3	8.65–9.75	Bt: 865–975 cm; brown (7.5 YR 5/4), silty clay, angular blocky microstructure, speckled and partially striated b-fabric, few clay coating, degraded calcite nodules, few Fe–Mn coating and hypo coating.
L 3	9.75–11.05	CBk: 975–1105 cm; brown (10 YR 5/4), silty clay loam, crystallitic and speckled b-fabric, cytomorphic calcite, needle-shaped calcite, calcite coating, shell fragments, few Fe–Mn coating, clay domain
P 4	11.05–12.95	Bt: 1105–1295 cm; dark reddish brown (7.5 YR 4/4), silty clay, angular blocky microstructure, channels and chambers, speckled and partially striated b-fabric, calcite depletion, common clay coating, common Fe–Mn coating and hypo coating, Fe–Mn nodules.
L 4	12.95–13.95	Ck: 1295–1395 cm; yellowish brown (10 YR 4/3), silty loam, speckled and crystallitic b-fabric, needle-shaped calcite, calcite nodules, calcite coating, shell fragments, very few Fe–Mn coating, few clay coating.
P 5	13.95–15.15	Bt: 1395–1515 cm; reddish brown (7.5 YR 4/3), silty clay, subangular blocky microstructure, channels and chambers, speckled and partially striated b-fabric, calcite depletion, common clay coating, common Fe–Mn coating and hypo coating, Fe–Mn nodules.
L 5	15.15–17	Ck: 1515–1545; 1605–1700 cm; yellowish brown (10 YR 6/4), silt loam, uniform, massive microstructure, crystallitic b-fabric, calcite nodules, calcite coating, few clay domains. CBk: 1545–1605 cm; brown (10 YR 4/6), silty loam, speckled and crystallitic b-fabric, needle-shaped calcite, calcite nodules, calcite coating, few Fe–Mn coating, few clay domain.
Aghband	~44	
Surface soil	0–0.5	A: 0–30 cm; yellowish brown (10 YR 5/4), silt loam, massive microstructure, without calcite depletion, root channels. Ck: >30 cm; yellowish brown (10 YR 6/4), silt loam, massive microstructure
Paleosol	40.5–42.5	Bwy-Bky-Bk: 40.5–42.5 m; brown (10 YR 6/4), slightly reddish hue, weakly developed subangular blocky, crystallitic and partially speckled b-fabric, few passage feature, gypsum mycelia.

Mobarakabad, the A horizon of the surface soil is strongly influenced by high calcite depletion, worm channels and excrement (fecal pellets) identified within a biopore associated with organic matter. The Bt horizon is characterized by clay illuviation and clay coatings (Fig. 4G). Calcite depletion zones can be identified as areas of speckled or striated b-fabric in a micromass dominated by a crystallitic b-fabric (Fig. 4H, I). The other noticeable characteristic pedofeature is Fe–Mn hydroxide nodules. Fe–Mn hydroxide nodules occur in volume percentages varying from about 10% in Bt horizons of P 3 (Fig. 4J) and P 4 (Fig. 4K) to 4% in surface soil and P 2.

Table 2
Micromorphological properties, MISECA and χ_{fd}% of B horizons at the sections.

Section	Horizon	Microstructure	B-fabric	Clay coatings	Decalcified zone	Alteration degree	Fe/Mn hydroxide	MISECA	Average χ_{fd}%
Mobarakabad									
Surface soil	Bt	Well separated abk	Speckled	Common	>90%	1	Few	15, moderately developed	9.0
P 1	Bk	Mod. separated abk to fine sbk	Speckled, partially crystallitic	Few	50–70%	1	Few	13, moderately developed	8.7
P 2	Bk	Mod. separated abk to fine sbk	Speckled, partially crystallitic	Few	50–70%	1	Few	12, moderately developed	8.5
P 3	Bt	Well. separated abk to sbk	Speckled, partially striated	Common	>90%	2	Common	18, well developed	10.0
P 4	Bt	Well separated abk	Speckled, partially striated	Common	>90%	2	Common	19, well developed	9.5
P 5	Bt	Well separated sbk	Speckled, partially crystallitic	Common	>90%	1	Common	16, moderately developed	3.1
Aghband									
Paleosol	Bwy	Weakly developed sbk	Crystallitic, partially speckled	–	20%	0	Very few	3, weakly developed	6.0
AG 2[a]	Bw	Weakly developed sbk	Crystallitic, partially speckled	–	20%	0	Very few	5, weakly developed	7.5

abk = angular blocky, sbk = subangular blocky.
[a] From Khormali and Kehl (2011).

https://doi.org/10.1016/j.yqres.2016.05.004 Published online by Cambridge University Press

Pronounced clay coatings occur in the Bt horizons of the surface soil, P 4 (Fig. 4K), and P 5 (Fig. 4L), which show abundant calcite depletion pedofeatures and some evidence of secondary calcite including pore infillings, coatings and hypocoatings. Mollusc shell fragments are dispersed throughout large parts of the deposit especially in loess horizons (Fig. 4M). Various forms of calcitic pedofeatures are present in loess horizons, most notable are calcite nodules, cytomorphic calcite and needle-fiber calcite. Most of the needles are randomly oriented or form subparallel bundles along the walls of vughs, although some parallel oriented needles are also observed (Fig. 4N). Micromorphological analysis showed that paleosols P 3 and P 4 have the highest MISECA values of 18 and 19 respectively, which reflect advanced soil formation. Conversely, P 1 (MISECA of 13) and P 2 (MISECA of 12) show the lowest degree of soil development (Table 2).

At Aghband, the microstructure of the horizons ranges from massive in the loess (Fig. 4O) to weakly developed subangular blocky in the paleosol. Fe–Mn hydroxide nodules are as little as 2% by volume percentages. The dominant b-fabric is calcitic crystallitic which indicates a low degree of soil formation. Most notable of the calcitic pedofeatures are microcrystalline impregnative gypsum mycelia. The paleosol shows a higher degree of soil formation, with MISECA of 3 compared to the loess deposits. The paleosol, AG 2 reflects a higher degree of soil development with MISECA values of 5 (Khormali and Kehl, 2011).

Magnetic susceptibility variations

The χ_{lf} and $\chi_{fd}\%$ – depth curve of the Mobarakabad section is shown in Fig. 5A. At Mobarakabad, χ_{lf} of the section ranges from 28 to 200 $\times 10^{-8}$ m^3 kg^{-1} and $\chi_{fd}\%$ varies from 0.36% to 11.39% with an average of 6.33% and $\chi_{fd}\%$ shows an approximately linear relationship with χ_{lf}. High MS values are present in the surface soil and the red-brown paleosols in which $\chi_{fd}\%$ values ranging from 8% to 11.4% and at the χ_{lf} peaks, $\chi_{fd}\%$ is often >11%. χ_{lf} for P 3 and P 1 have the highest and second highest values in the section respectively. However, χ_{lf} and $\chi_{fd}\%$ of the P 5, with a respective mean of 51 $\times 10^{-8}$ m^3 kg^{-1} and 3% are significantly lower than the surface soil and other paleosols. In contrast, low MS values are present in the loess horizons and the lowest value is present in the Ck horizon of L 1 with an average χ_{lf} of 31 $\times 10^{-8}$ m^3 kg^{-1} and $\chi_{fd}\%$ of 2.5%. Among the loess horizons, L 3 shows highest χ_{lf} and $\chi_{fd}\%$ with an average of 67 $\times 10^{-8}$ m^3 kg^{-1} and 8.7% respectively. A MS increase is seen in the CBk horizons of L 1, L 2 and L 5 compared to their Ck horizons.

The χ_{lf} of the Aghband loess (Fig. 5B) is significantly lower than that of Mobarakabad in that χ_{lf} is mostly less than 30 $\times 10^{-8}$ m^3 kg^{-1} with an average of 24 $\times 10^{-8}$ m^3 kg^{-1} and low values are especially present in the loess. Moreover, the $\chi_{fd}\%$ of the Aghband loess is mostly <3% with an average of 1.8%. In this section, the maximum χ_{lf} (40 $\times 10^{-8}$ m^3 kg^{-1}) and $\chi_{fd}\%$ (6.8%) are seen in the paleosol. The maximum χ_{lf} and $\chi_{fd}\%$ of the AG 2 paleosol are 80 $\times 10^{-8}$ m^3 kg^{-1} and 8.8% respectively, which is considerably higher than of the paleosol.

CBD extractable iron (Fe_d)

Fe_d values are distinctly higher in paleosols than loess in both sections (Fig. 5). At Mobarakabad, the content of Fe_d ranges from 4.3 mg/gr in L 1 to 10.75 mg/gr in P 5 (Fig. 5A). The curve of Fe_d and χ_{lf}/Fe_d mirror the χ_{lf} and $\chi_{fd}\%$ curves and the correlation coefficients (r^2) for Fe_d and χ_{lf} and for Fe_d and $\chi_{fd}\%$ in P 3 with values of 0.663 and 0.703 respectively are higher than the other loess and paleosol horizons. However, in P 5 the curve of Fe_d differs from χ_{lf} and $\chi_{fd}\%$ (Fig. 5A). In contrast, at the Aghband section the content of Fe_d varies from 1.95 mg/gr in the loess to 4.4 mg/gr in the paleosol. The Fe_d and χ_{lf}/Fe_d curves of the section are similar to the χ_{lf} and $\chi_{fd}\%$ curves (Fig. 5B) and Fe_d values are significantly positively correlated with $\chi_{fd}\%$ at $P < 0.01$ level ($r^2 = 0.301$).

Calcium carbonate equivalent (CCE) analysis

In Mobarakabad, CCE varies between 0.5 and 40%, with lower values in paleosols and higher values in loess horizons (Fig. 5A). Also the upper parts of L 2, L 3 and L 4 are recalcified and enriched in $CaCO_3$ as shown by the highest $CaCO_3$ contents of 40%, 38% and 37% respectively. In contrast, at Aghband CCE varies between 15 and 20% (Fig. 5B) and there is no significant difference in CCE between the paleosol and loess. As shown in Fig. 5, a negative relationship was observed between MS and CCE in these sections.

Mineralogical analysis

XRD patterns and the mineralogical composition of the clay fraction are shown in Fig. 6 and Table 3. XRD patterns of the oriented samples of the clay fraction exhibited the presence of illite (peaks around 1.0 nm), smectite and illite-smectite mixed layers (weak and broad peak around 1.7 nm) and traces of quartz (small peak at 0.425 nm). The peak at 1.4 nm is attributed to vermiculite and chlorite since the 1.4 nm peak decreased and shifted to lower d-spacing resulting in the increasing intensity of the 1.0 nm peak after K-25°C and a peak at approximately 1.4 nm remained after K-550°C. The peak at 0.72 nm is attributed to kaolinite and chlorite because the peak was absent in K-550°C and separated with the use of the 0.358 nm peak (kaolinite) and the 0.354 nm peak (chlorite). The clear peak at 1.23 in K-550°C indicated that the interlayer of the irregularly interstratified mica and vermiculite minerals was occupied by Al polymers (Egli et al., 2004). At Mobarakabad, illite is the dominant clay mineral with lesser amounts of chlorite, smectite, kaolinite, vermiculite and hydroxy-interlayer vermiculite (Table 3). Kaolinite concentration is higher in loess horizons than in paleosols. Vermiculite is present in the Bt horizons of the surface soil (Fig. 6A), P 3, P 4 and P 5 (Fig. 6B) and hydroxy-interlayer vermiculite is present in small amounts in the Bt horizons of the surface soil and P 4. Smectite is present with small amounts in loess horizons (Fig. 6C) and increases in paleosols (Fig. 6A). Chlorite content is higher in loess horizons and significantly decreases in the surface soil and paleosols (Table 3). At Aghband, the clay fractions of the samples are dominated by illite and chlorite but also contain some smectite and kaolinite with highest content for illite and lowest for smectite (Fig. 6D and Table 3).

Discussion

Paleoclimatic implications of the loess-paleosol sequences in north Iran

Micromorphological features of paleosols such as clay illuviation, calcification, decalcification, redoximorphosis or relocation, reflect the environmental conditions under which these soils formed (Bronger et al., 1994; Kemp, 1998; Fedoroff et al., 2010; Meier et al., 2014). At the Mobarakabad section, a comparison of the degree of soil development of the surface soil and paleosol Bt horizons, using MISECA, indicates that the Bt horizons of P 3 and P 4 have the highest degree of development including Fe–Mn nodules and the best developed and preserved clay coatings (Fig. 4J and K). These features may reflect higher soil moisture, strong enrichment in clay particles due to clay neoformation and clay illuviation from overlying horizons as evidenced by clear clay coatings and dominance of vermiculite (Table 3) and therefore may indicate high

https://doi.org/10.1016/j.yqres.2016.05.004 Published online by Cambridge University Press

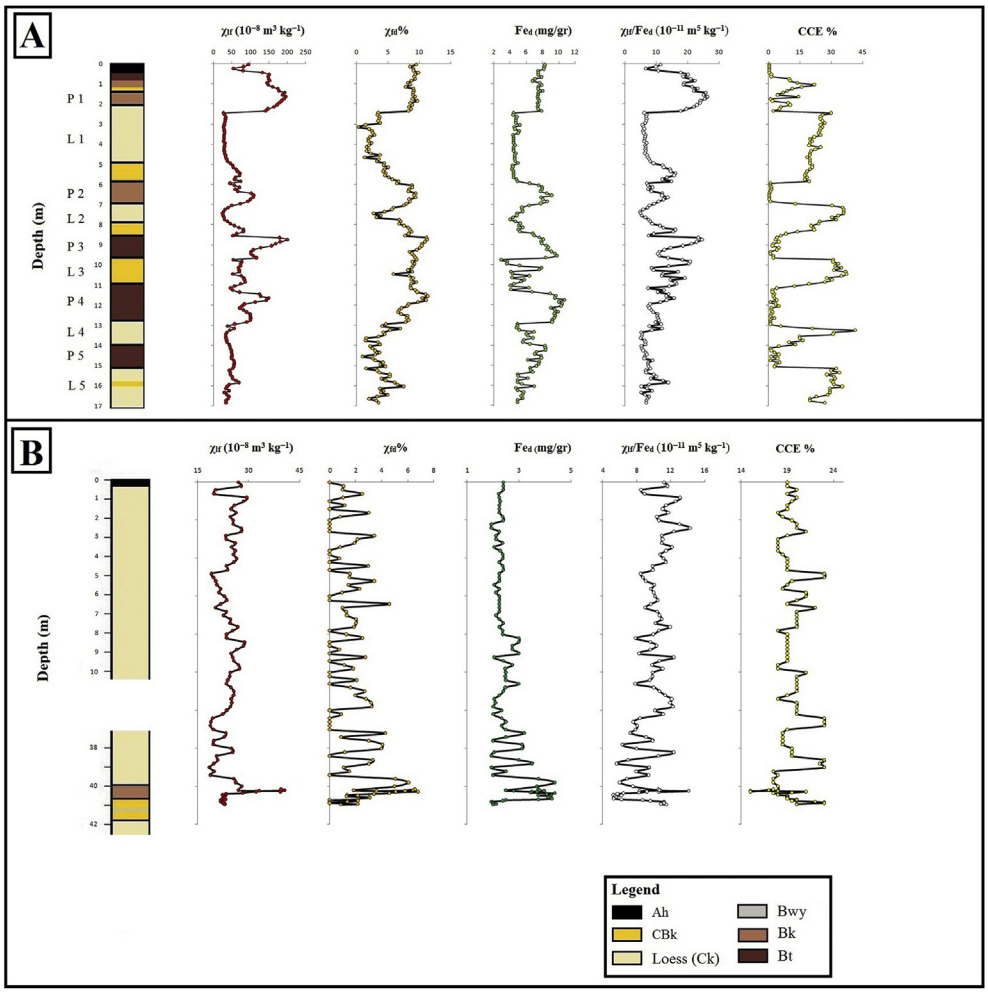

Figure 5. The χ_{lf}, χ_{fd}%, Fe_d, CCE and χ_{lf}/Fe_d – depth curve of the sections; Mobarakabad (A), Aghband (B).

precipitation during their formation. Moreover, micromorphological analyses and the pattern of χ_{fd}% variations in the sections indicate a positive relationship between MISECA and χ_{fd}% (Table 2). The maximum average χ_{fd}% values are 9.5 and 10 in P 4 and P 3 respectively that suggest pedogenesis in these paleosols was stronger than in the surface soil and in other paleosols. Micromorphological analyses also confirm that these paleosols are well developed with a MISECA of 19 and 18 respectively.

The limited expanding nature of the vermiculitic type of clay minerals and the stable landscape on which the soil formed provided a suitable environment for the downward translocation of clay and thus formation of thick and more pronounced clay coatings with higher soil moisture conditions. Moreover, with intense chemical weathering conditions, hydroxy-interlayer vermiculite can be formed (Khormali and Abtahi, 2003) and is present in small amounts in the Bt horizons of the surface soil and of P 4. Similar results were reported by Khormali and Kehl (2011) in Bt horizons of Alfisols in humid regions (MAP > 850 mm) of Northern Iran. In the sections, higher kaolinite concentrations in loess horizons compared to paleosol horizons indicate that the presence of this mineral is mainly controlled by source area mineralogy rather than pedogenesis. Khormali and Kehl (2011) suggest that increasing available moisture in soil, and consequently the intensity of leaching increases the release of K from micaceous minerals and especially illite. A calcareous environment with high Mg^{2+} and high Si^{4+} mobility may provide favorable conditions for the formation of smectite through transformation. Hence, compared to Aghband and loess horizons in Mobarakabad, the increase in smectite in Bt horizons of the Mobarakabad section (Table 3) may be mainly of transformed origin.

Illite and chlorite are the dominant clay minerals in northern Iranian loess and may carry environmental information (Khormali and Kehl, 2011). Illite is not easily weathered in warm and wet conditions, whereas chlorite is very susceptible to weathering (Zhao et al., 2005). Neither illite nor chlorite is formed pedogenically in the loess sequences; they are considered to be derived from preexisting sediments and from very low- to low-grade metamorphic rocks (Liu et al., 1985; Ji et al., 1999). Chlorite is found in all samples with different amounts (Ghafarpour et al. unpublished diffuse reflectance spectrophotometery data) and since the reflection at 1.4 nm remains stable after saturation with K^+ heating to 550°C, it is very likely, that it is primary chlorite of detrital origin. XRD data shows that chlorite easily weathered in the wetter conditions of paleosols. Compared to loess horizon, the chlorite content is significantly lower in the surface soil and paleosols. Previous studies show that the silicate weathering in loess and paleosols are mainly characterized by the change of chlorite to vermiculite and/or smectite (e.g., Zhao et al., 2005). Chlorite together with vermiculite occurs in the Bt horizon of surface soil, P 3, P 4 and P 5. Also, the significant decrease in the content of chlorite in the

https://doi.org/10.1016/j.yqres.2016.05.004 Published online by Cambridge University Press

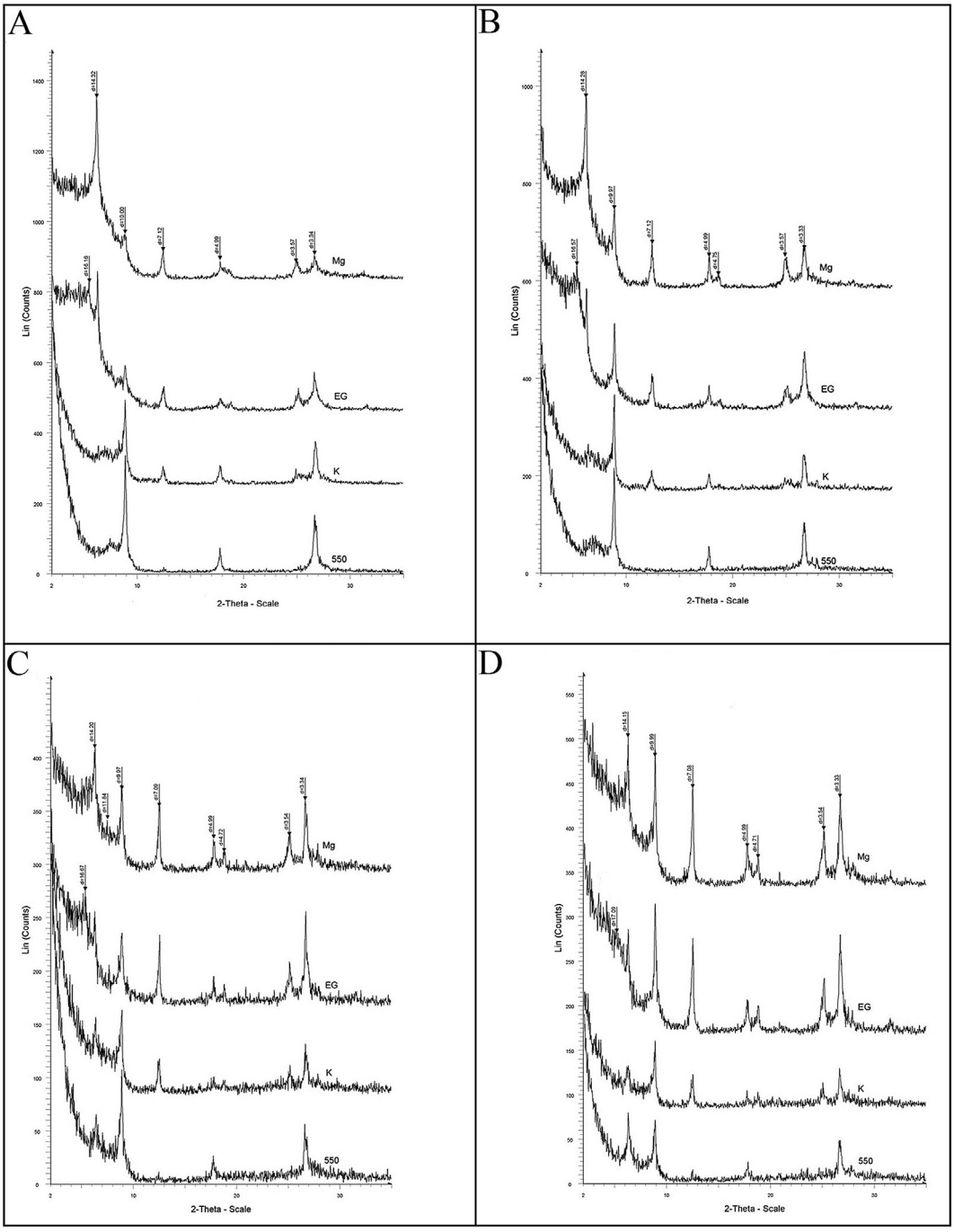

Figure 6. X-ray diffractograms of the clay fraction in Bt horizons of surface soil (A), P 5 (B) and Ck horizon of L 1 (C) at Mobarakabad and in loess deposits (D) at Aghband section.

surface soil and paleosols (Table 3) coupled with CBD and MS increase (Fig. 5A) suggests a wetter climate during their formation and indicates that strong chlorite weathering was likely due to higher precipitation. As the main iron-bearing silicate mineral, the weathering of chlorites may also provide free iron for the production of nanoscale iron oxide minerals in the pedogenic process (Ji et al., 2002; Liu et al., 2005), leading to the enhancement of the CBD (Guo et al., 2000) and magnetic susceptibility (Maher, 1998; Ji et al., 2002) in paleosols. Our data therefore corroborates the views of Zhao et al. (2005) and Ji et al. (2002) that during weathering chlorite may release iron, so that nanometer-sized iron oxide minerals may form, and the pedogenic free Fe_2O_3 and magnetic susceptibility increased in the paleosols. Therefore we suggest that weathering of chlorite can be a good indicator of a strongly humid climate during the formation of loess-paleosol sequences in Northern Iran. This conclusion is similar to the results presented by Khormali and Kehl (2011) which indicated that the modern soil characteristics show a strong correlation with precipitation along the pronounced climate gradient in Northern Iran and that the content of chlorite decreased due to increased humidity from east to west and from north to south on the Iranian loess plateau.

Primary carbonates, identified as a main component of the sediments deposited in the loess-soil sequences of the Caspian Lowland and loess deposits in northern Iran have contents of

https://doi.org/10.1016/j.yqres.2016.05.004 Published online by Cambridge University Press

Table 3
Semiquantitative analyses of clay minerals in the studied sections.

Section/horizon	Illite	Chlorite	Kaolinite	Smectite	Vermiculite	Hydroxy-interlayered vermiculite
Aghband						
Surface soil	+++	++	++	+	−	−
Paleosol (Bwy)	+++	++	++	+	−	−
Loess	++++	+++	++	+	−	−
Mobarakabad						
Surface soil						
A	+++	++	++	++	−	−
Bt	++	+	+	++	++	+
P 1	++	++	++	++	−	−
L 1	++++	+++	++	+	−	−
P 2	+++	++	+	++	−	−
L 2	+++	+++	++	+	−	−
P 3	++	+	+	++	++	−
L 3	+++	++	+	++	−	−
P 4	++	+	+	++	++	+
L 4	+++	++	++	+	−	−
P 5	++	+	+	++	++	−
L 5	+++	+ +	+	+	−	−

++++: >50%; +++: 30–50%; ++: 10–25%, +: <10%, −: not present.

primary $CaCO_3$ ranging between 15 and 20% (Frechen et al., 2009; Khormali and Kehl, 2011). In the Aghband section, CCE varies between 15 and 20%, which might primarily be geologic in origin. At Mobarakabad, very low values of CCE in paleosols indicates that high precipitation and carbonate leaching occurred during their formation. Carbonate content largely depends on the balance between precipitation-induced leaching intensity and temperature-related evapotranspiration effectiveness (Reheis, 1987). In Mobarakabad, relatively higher values of CCE in loess horizons may indicate that decreased evapotranspiration probably caused soil moisture to increase and may have permitted some carbonate to be leached from the soils, driving the carbonate enrichment in the underlying loess layers. The rather high carbonate content and its fluctuations can show connections with the extensive leaching of the overlying pedocomplex and/or it may be influenced by the changes of source material of the dust (Barta, 2014). The upper parts of L 2, L 3, and L 4 are enriched in $CaCO_3$, indicating that the carbonate in the parent material could not be the only source of carbonates and the loess horizons were strongly influenced by precipitation of secondary carbonates leached from the overlying horizons (paleosols) due to high leaching and/or they may indicate paleoenvironmental changes leading to slightly less arid (more moist) conditions and leaching during their formation.

Carbonate concretions (also known as loess dolls) are macroscale secondary carbonates and are frequently found below paleosols because they are formed by leaching and re-precipitation (Jiamao et al., 1997; Kemp, 1998; Barta, 2011). The presence of large loess dolls in L 5 (Fig. 4F) may be related to former stable surfaces developed under decreasing dust accumulation rates, variable moisture regimes and may indicate paleoenvironmental changes connected with a multiphase leaching history.

Microscale secondary carbonates include calcified root cells, hypocoatings, carbonate coatings, earthworm biospheroids, and needle-fiber calcite (Barta, 2014). The origin of needle-fiber calcite is related to fungal biomineralization or physiochemical precipitation from supersaturated solutions (Verrecchia and Verrecchia, 1994; Khormali et al., 2006; Cailleau et al., 2009). Needle-fiber calcite indicates the presence of decaying organic material, because these pedofeatures appear in former humic horizons where fungi were associated with higher plants and took part in the decomposition processes (Verrecchia and Verrecchia, 1994; Bajnóczi and Kovács-Kis, 2006). Their occurrence in loess indicates a vegetation cover and seasonally sufficient moisture for saprophyte activity (Becze-Deák et al., 1997). In Mobarakabad, the absence of needle-fiber calcite, clay coatings, and lower values of $\chi_{fd}\%$ and χ_{lf} in the Ck horizon of L 1 indicate cold and dry conditions during its accumulation. In contrast, the existence of needle-fiber calcite (Fig. 4N), few clay coatings, speckled b-fabric and higher values of $\chi_{fd}\%$ and χ_{lf} in L 2, L 3, L 4 and L 5 and the CBk horizon of L 1 indicate some degree of pedogenesis and suggest comparatively semi-arid conditions during or after dust accumulation because these horizons show stronger pedogenic features than the Ck horizon of L 1.

Ferruginous mottles are typically a product of alternating oxidation and reduction conditions during soil formation associated with gleying under water-saturated conditions (Chlachula, 2003). Ferruginous mottles are widespread in the Mobarakabad section. There are more ferruginous mottles in paleosols than the loess because the air and water permeability of loess is better than the soil due to its coarser texture (Chen et al., 2015). The high volume percentages of Fe–Mn nodules and mottles in P 3, P 4 and P 5 also indicate that high precipitation and alternating oxidizing and reducing conditions occurred during their formation. In contrast, at Aghband the lack of calcite nodules, Fe–Mn mottles, clay coating and low values of $\chi_{fd}\%$ and χ_{lf} suggest that the degree of weathering and pedogenesis and the translocation of clays was weaker than that of Mobarakabad.

The presence of gypsum in silty deposits in north and north eastern Iran has been noted by researchers (Frechen et al., 2009; Karimi et al., 2011; Khormali and Kehl, 2011). The likely source of the gypsum in loess deposits at Aghband is the thick beds of the green and black shale and marly limestone in the Aghband fault zone (Karimi et al., 2009). Occurrence of gypsum in paleosols at Aghband may indicate that local climatic conditions with low precipitation and high evaporation did not allow leaching of soluble gypsum during soil formation.

Enhancement mechanisms of magnetic susceptibility in the sections

Several possible mechanisms for magnetic enhancement have been suggested for the Chinese Loess Plateau. These include aeolian dust dilution (Kukla and An, 1989), sediment compression and carbonate leaching (Heller and Tungsheng, 1984), decomposition of plant residues (Meng et al., 1997) and pedogenesis (Zhou et al., 1990; Maher, 1998). Another model for magnetic enhancement is the wind velocity/vigor hypothesis (also named the Alaskan or

https://doi.org/10.1016/j.yqres.2016.05.004 Published online by Cambridge University Press

Siberian model), where wind strength affects magnetic susceptibility values of loess through physical sorting of magnetic grains (Begét and Hawkins, 1989). One of the most widely accepted interpretation of the loess magnetic susceptibility enhancement is in situ formation of ultrafine magnets during pedogenesis (i.e., pedogenic model), which suggests that the magnetic enhancement is the result of the formation of ultrafine (superparamagnetic (SP) and single domain (SD)) magnetic minerals during the pedogenic process (Liu et al., 2007, 2008; Song et al., 2010a).

The magnetic susceptibility of the studied sections shows a general positive proportional relationship to the modern climate which can be used as a proxy for paleoprecipitation. The Aghband section is much closer to the desert, with altitude (150 m asl) with MAP of 300 mm, whereas the Mobarakabad section has a relatively high altitude (310 m asl) with MAP of 670 mm. This indicates that the relationship between the MAP and pedogenic intensity can explain the MS enhancements in Mobarakabad. When climate varies toward higher temperature and higher moisture, weathering and pedogenesis also increase, which favors the development of an oxidizing pedogenic environment, forming ultrafine magnet grains such as maghemite and magnetite in this oxidizing environment, resulting in an increase of magnetic susceptibility (Song et al., 2010a). In Mobarakabad, high χ_{lf} together with high χ_{fd}% indicate that many extrafine grains of maghemite and magnetite might have been formed during pedogenesis under warm, moist paleoclimates. The contributions of magnetite to magnetic susceptibility in the Iranian loess can be ignored because the mass magnetic susceptibility of pure SD magnetite is 450×10^{-6} m^3/kg (Song et al., 2010a) which is at least 225 times that of the highest Iranian loess MS (i.e. 2×10^{-6} m^3/kg). Therefore, loess magnetic susceptibility enhancement in paleosols at Mobarakabad probably mainly depends on the content of maghemite. Song et al. (2010a) assumed that warm humid climates are favorable to form new fine-grained magnetic minerals, and strong pedogenesis produces new magnetic minerals. The increased precipitation is conducive to chemical weathering and biological processes and pedogenesis. Therefore, the pedogenic model can explain the MS enhancements of the Mobarakabad section.

χ_{fd}% is usually regarded as a proxy to determine the contribution of superparamagnetic particles to magnetic susceptibility (Zhou et al., 1990; Liu et al., 1990, 1992), which indicates that the content of super-paramagnetic particles is very low, and is a very limited contributor to the susceptibility enhancements. χ_{fd}% is also related to the formation of new pedogenic ferromagnetic minerals and is higher in paleosols than in loess (Chlachula et al., 1998; Kravchinsky et al., 2008). χ_{fd}% of the Mobarakabad section shows an approximately linear relationship with χ_{lf} and χ_{fd}% in paleosols being higher than in loess horizons within the section, which reflects a strong pedogenesis. The average χ_{lf} and χ_{fd}% values of the Aghband section are much lower than those of Mobarakabad section, indicating that the total magnetic mineral concentration of the northern Iranian loess plateau is less than that of the loess in the southern basin (foothills of Alborz Mountains). This may be caused by differences such as altitude, or the distance to dust source regions. Dry climate conditions in Aghband give rise to weaker pedogenic processes in loess, which are unfavorable to producing SP magnetic grains so that the SP grains have a very limited contribution to magnetic enhancement. Hence, the main contributors to magnetic susceptibility may be pseudo-single-domain maghemite and multi-domain magnetite, which are difficult to produce during the process of pedogenesis (Song et al., 2010a) and therefore they may originate partially at least from detrital magnetic minerals from the source region.

These findings therefore lead to the conclusion that different behaviors of magnetic susceptibility between the Aghband and Mobarakabad loess sections are mainly produced by their different pedogenic environments, which are in turn related to local topography and climatic conditions. With a median grain size of 29 μm, the loess from Aghband is considerably coarser than the loess from foothills of Alborz Mountains (Frechen et al., 2009). Also, the content of clay, silt and sand for the modern loess deposits in Aghband are 18%, 72%, and 10% respectively whereas L 1 in Mobarakabad consists of about 33% clay, 57% silt and 10% sand. This may indicate higher wind velocities during the time of deposition and/or proximity to a sediment source in the Aghband section and may indicate weak biological and chemical weathering processes. The exact location(s) of the various potential loess source area(s) in northern and northeast Iran are still debated (Frechen et al., 2009; Kehl, 2009; Karimi et al., 2011), however, XRD analyses and MS of L1 in the Mobarakabad section and modern loess deposits in the Aghband section are similar, and therefore they probably have a similar source.

Magnetic susceptibility is regarded as a proxy of paleoprecipitation (Heller et al., 1993; Maher et al., 1994; Maher and Thompson, 1995; Evans et al., 2002). It is also believed that magnetic susceptibility is related to local precipitation because of the difference of topography (e.g., altitude, slope) (Song et al., 2010a). In Aghband, the CCE, Fe_d and XRD analyses of the paleosol are similar to the AG 2 paleosol (Khormali and Kehl, 2011) even though the sections differ in MS. The χ_{lf} of the AG 2 paleosol (80×10^{-8} m^3 kg^{-1}) is higher than of the studied paleosol (40×10^{-8} m^3 kg^{-1}). Also, the paleosol shows a lower degree of soil formation, with MISECA of 3 and χ_{fd}% values of 6, than AG 2 which reflects a higher degree of soil formation with MISECA and χ_{fd}% values of 5 and 7.5 respectively (Table 2). We therefore postulate that a difference in rainfall values is probably responsible for the increase in MS seen in AG 2 and these two paleosols may belong to different time periods in the past and be formed under different precipitation regimes and/or receiving different local precipitation because of the difference of slope.

Magnetic depletion in the P 5 at Mobarakabad

As shown in Fig. 5A, χ_{lf} of the P 5 is greatly reduced, whereas, the Fe_d values remain at high levels. Fe_d represents the amount of fine-grained secondary Fe oxides in soils (Mehra and Jackson, 1960). The total Fe_d may indicate the degree of pedogenesis and the χ_{lf}/Fe_d ratio reflects the proportion of ferrimagnetic minerals (FM) to total secondary Fe oxides (Hu, 2004; Hu et al., 2009a,b). Higher Fe_d and lower χ_{lf}/Fe_d in P 5 indicate lower FM in the secondary Fe oxides and it seems unlikely that primary deposition could influence Fe oxide mineralogy. Kravchinsky et al. (2008) assumed that gleying, acidification and podzolisation may cause MS to decrease by destroying original magnetic minerals and/or by limiting the formation of secondary ferromagnetic minerals in west Siberian loess sections. Based on detailed rock magnetism research, Liu et al. (2008, 2012) inferred that extreme moist and cold conditions during interglacial periods in Siberia and central Alaska, tended to produce a moist-oxidizing to reducing environment, which led to the formation of weakly magnetic iron oxyhydroxides and sulfides and that reduction of ferromagnetic minerals to weakly magnetic iron oxyhydroxides and sulfides can effectively deplete the MS value. Interglacial periods may favor more saturated soils and stronger moist-oxidizing conditions. If moisture is over a critical value, the pedogenic environment tends towards a moist-oxidizing – reducing condition, that would result in greater destruction of iron oxides (maghemite and magnetite) to form more stable iron oxyhydroxides (such as goethite). Further moisture causing soil saturation (gleying) would lead to destruction of iron oxides to form iron sulfides. In both the above processes, the iron oxides

https://doi.org/10.1016/j.yqres.2016.05.004 Published online by Cambridge University Press

deposited by aeolian dust are destroyed and the more paramagnetic minerals are produced, leading to a negative relationship between magnetic susceptibility with pedogenesis. However in the most cases, the loess susceptibility will bear no relation to paleoclimate or pedogenesis, due to pedogenic moisture that varies around a critical value (Liu et al., 2008).

Micromorphological studies show oriented clay films, Fe–Mn hydroxide and indicate that paleosol P5 is moderately to well developed, with a MISECA of 16 (Table 2). The content of clay, silt and sand for Bt horizon of the surface soil are 45%, 41%, and 14%; for P 3: 40%, 53%, 7%; for P 4: 46%, 40%, 14% and 43%, 43%, and 14% for P 5, indicating there is no major difference in the texture among these soils. Moreover, there is no evidence for existence of ground water fluctuation in the section. In anaerobic soil conditions, pedogenic fine maghemite and/or magnetite are easily reductively dissolved (Cornell and Schwertmann, 2003), causing the depletion of soil magnetism (Maher, 1998; Grimley and Arruda, 2007). Hu et al. (2009a,b) assumed during post-depositional hydromorphic processes, pedogenic maghemite was more easily dissolved than hematite, which caused the sharp decrease of χ_{lf}. Therefore, temporary anoxic conditions could have occurred in P 5 due to high precipitation and maghemite may have been completely destroyed, but hematite, as indicated by reddish hue (Ghafarpour, A. et al. unpublished diffuse reflectance spectrophotometery data) and Fe_d has not been significantly affected. Hence, the χ_{lf} of this horizon may have been initially higher and decreased later. As a result, the χ_{lf} of P 5 is inconsistent with its strong degree of pedogenesis. The inconsistency between weak magnetism and intensive weathering degree in loess sequences has previously been observed by Liu et al. (1999, 2001), Sun and Liu (2000), Hu et al. (2003, 2009a,b) and explained by Balsam et al. (2004, 2011). Higher precipitation is also indicated by high chlorite weathering, dominance of vermiculite, and a sharp decrease in MS in P 5 suggesting a very wet climate during the formation of P 5.

Liu et al. (2003) suggested that, if soil moisture exceeds some critical level and Fe reducing bacteria are present, FM will be dissolved and the correlation between pedogenesis and χ_{lf} in loess deposits may be uncertain. A similar result was also reported by Hu et al. (2009a,b) who indicated that χ_{lf} can be used as a paleoclimatic proxy only when the amount of FM is significantly correlated with the degree of soil development. Our study showed that a decrease in MS in P 5 at the Mobarakabad section, due to temporary anoxia resulting from stagnant water from very high precipitation may indicate wet conditions during soil formation. Our work therefore corroborates Liu et al. (1999, 2003, 2008), Song et al. (2010a) and Balsam et al. (2004, 2011) that there is not a linear relationship between MS and pedogenesis. Moreover, when temporary anoxic conditions due to groundwater fluctuations or higher precipitation occur, the correlation between MS and pedogenesis in loess-paleosol sequences can be complicated and uncertain. Our results are also consistent with Shi (2005), Song et al. (2008, 2010b), Jia et al. (2011, 2012) and Chen et al. (2012, 2015) that pedogenic enhancement, pedogenic depletion and geographic locations should all be taken into account when explaining the observed variations in the magnetic parameters.

Comparison of the magnetic susceptibility of Iranian loess with other regions

Magnetic susceptibility values are affected by sediment sources, sedimentary processes, post-depositional pedogenesis, weathering processes, and biological effects. Therefore, the MS enhancement mechanism of loess-paleosol sequences in different regions may vary significantly (Zhu et al., 2000; Wang et al., 2003; Liu et al., 2007). In the Iranian loess, low χ_{lf} together with low χ_{fd}% in loess, and high χ_{lf} with high χ_{fd}% in paleosols, indicates the formation of SP/SD grains during pedogenesis. In the northern Black Sea coastal area (Dodonov et al., 2006) Tajikistan (Ding et al., 2002; Yang et al., 2006), Romania (Constantin et al., 2014) and Chinese loess (Liu et al., 1990; Zhou et al., 1990) the relationship between MS and pedogenesis is very close to that of Iranian loess (Table 4). However, in Alaska and the Kurtak section in Siberia, loess intervals generally have higher susceptibility compared to the paleosols (Liu et al., 1999, 2001, 2008; Zhu et al., 2003).

The average MS values of the Mobarakabad section are much lower than the Chaona section located in the central Chinese Loess Plateau, greater than the Zhaosu section and similar to the Talede section the Ili Basin in eastern Central Asia (Table 4). This indicates that the total amount of magnetic minerals in the Iranian loess sediments is much lower than in Chinese loess, but higher than of the Zhaosu section and is close to the Talede section, which means that the total amount of magnetic minerals in the Mobarakabad section is similar to the eastern Ili Basin (Talede section). Also, the maximum values of χ_{lf} in paleosols at Mobarakabad are higher than those of in Romania, Tajikistan and the northern Black Sea coastal area (Table 4). However, χ_{lf} in the loess horizons of Mobarakabad is similar to those of the northern Black Sea coastal area. While χ_{lf} in the loess horizons of Mobarakabad is approximately the same as that of the northern Black Sea coastal area, χ_{lf} in the surface soil P 1, P 3 and P 4 in Mobarakabad is higher than those in the northern Black Sea coastal area. At present, the MAP at the Roksolany section in the northern Black Sea coastal area is about 470 mm, which is drier than Mobarakabad (MAP of 670 mm). This indicates that the climatic gradient as observed in the area of the Mobarakabad section might have existed in the late Pleistocene and indicates a wetter climate in the Mobarakabad region compared to the northern Black Sea coastal area during the Upper Pleistocene.

In contrast, the average χ_{lf} value of the loess in the Aghband section is much lower than that in Ili and Chinese loess (Table 4), which means that the total amount of magnetic minerals in Aghband and the Iranian loess plateau with low precipitation, is much lower than that in that in Ili and Chinese loess. However at Aghband the MS characteristic in loess is comparable with those at northern Black Sea coastal area (Table 4), indicating that the occurrence and transport of atmospheric dust in northern Iran may be similar to that in the northern Black Sea coastal area.

Stratigraphic comparison with other palaeoclimatic archives

Figure 7 summarizes correlations between the loess stratigraphy of different sites in northern Iran. Based on the MS variation, the formation of P 1 in the Mobarakabad section may be correlated to the first Bt-horizon in the Toshan section (Vlaminck et al., 2015) and the Bryansk paleosols (26,760 ± 7240 yr BP) in the Rokolany section in the northern Black Sea coastal area (Dodonov et al., 2006). Based on the aforementioned assumption, the absence of developed paleosols with same age at the Chashmanigar section (Ding et al., 2002) in Tajikistan may indicate that during MIS 3, the southern and western Iranian loess plateau had experienced a warmer and wetter climate than in Tajikistan. Also, L 1 at Mobarakabad indicates a period of increased dust deposition with lower values of MS in the Ck horizon and only minor soil formation with MS enhancement in the CBk horizon and may indicate a transition from MIS 4 to MIS 3. This may corroborate the results of Frechen et al. (2009) who proposed increased dust accumulation starting at around 60 ka for loess at the Neka section and Vlaminck et al. (2015) who assumed that Unit 4 at Toshan represents a transition from MIS 4 to MIS 3 (see Fig. 7), based on luminescence ages that range from 66 ± 4.7 to 52.4 ± 3.5 ka (see also Lauer et al., 2015). Because of the lack of chronological data, the pedostratigraphical correlation of P 2 to L 5 at Mobarakabad with the other previously studied sections in Northern Iran is less clear.

https://doi.org/10.1016/j.yqres.2016.05.004 Published online by Cambridge University Press

Table 4
Magnetic susceptibility data used in this study.

Section	Location	χ_{lf} (10^{-8} m^3 kg^{-1})			χ_{fd}%			
		Min	Max	Mean	Min	Max	Mean	
MS of studied sections								
Mobarakabad	Iran	28	200	76	0.36	11.39	6.33	
Aghband	Iran	18	40	24	0.00	6.81	1.80	
MS of previously studied sections used in this study								Reference
Costineşti	Romania	~20	~150	–	–	–	–	Constantin et al., 2014
Northern Black Sea coastal area	Ukraine	15	120	–	–	–	–	Dodonov et al., 2006
Chashmanigar	Tajikistan	~20	~150	–	–	–	–	Ding et al., 2002
Zhaosu	Ili Basin	–	–	54.30	1.33	6.07	2.90	Song et al., 2010a
Talede	Ili Basin	–	–	76.90	1.33	6.07	2.90	Song et al., 2010a
Kurtak	Siberia	115	300	–	0.19	2.92	–	Liu et al., 2008
Chaona	China	–	–	116.80	7.50	12.10	–	Song et al., 2010a

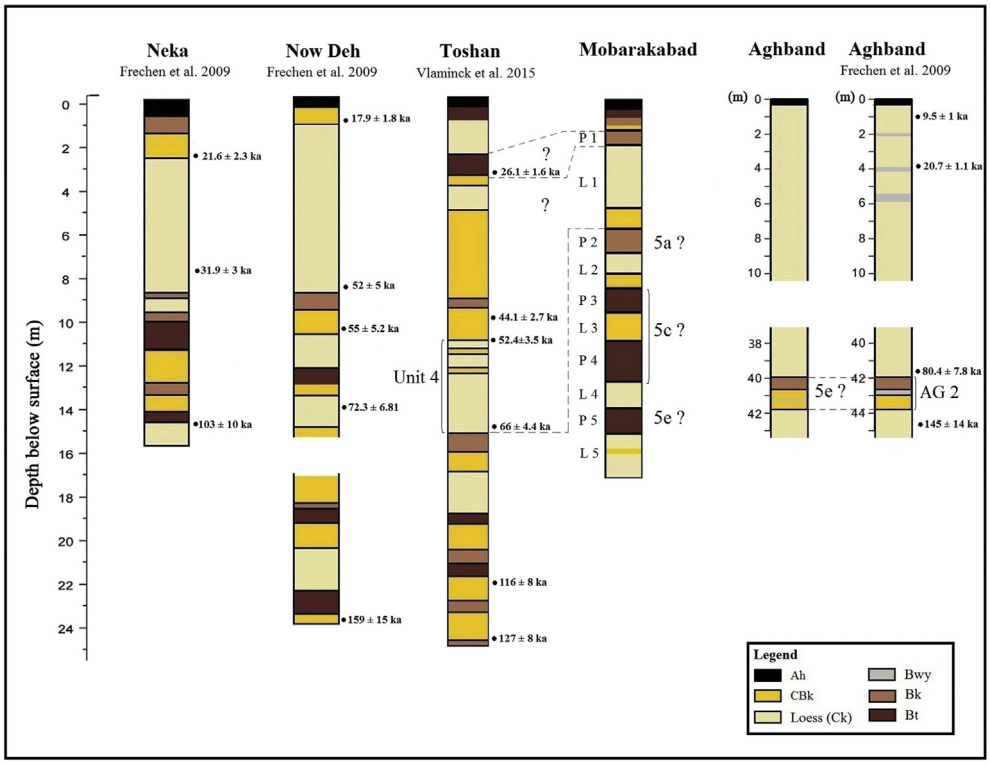

Figure 7. Preliminary pedostratigraphic correlation of Mobarakabad and Aghband section with loess-paleosol sequences in Northern Iran (Frechen et al., 2009; Vlaminck et al., 2015).

Frechen et al. (2009) assumed that the developed paleosol at the Aghband section (Ag 2) likely correlates with MIS 5e, the last interglacial. Therefore, we postulate that the paleosol at Aghband most likely correlates with MIS 5e and is in good agreement with the findings of Frechen et al. (2009) for AG 2 (see Fig. 7). However as discussed above their significant MS difference should be taken into account and a chronostratigraphic correlation of loess and paleosols at Mobarakabad and Aghband with the aforementioned archives requires age control by means of a luminescence dating study.

Conclusions

At the Mobarakabad section, based on the degree of soil development of surface and paleosol Bt horizons and taking MISECA into account, it appears that the Bt horizons of P 3 and P 4 have the highest degree of development. The presence of Fe–Mn nodules, vermiculite and high values of χ_{lf} and χ_{fd}% indicate high precipitation during their formation. Post-depositional processes may increase the MS value by producing new ferromagnetic minerals during oxidation of well aerated soils and also decrease the MS value by reducing processes (Chen et al., 2015). In P 5 even higher precipitation is indicated by chlorite weathering, the dominance of vermiculite and a sharp decrease in MS suggesting very wet conditions. Our study demonstrates that once the loess material is deposited pedogenesis is the dominant factor affecting variation of magnetic mineralogy and susceptibility. This study has also suggested that the susceptibility may be a complicated parameter; its application as a proxy of paleo precipitation has its limitations and conditions and therefore more attention should be paid to topography, depositional environment, and climatic factors, when loess magnetic properties are used for paleoclimate reconstruction (Liu et al., 2008).

https://doi.org/10.1016/j.yqres.2016.05.004 Published online by Cambridge University Press

Acknowledgments

We would like to acknowledge Gorgan University of Agricultural Sciences and Natural Resources, Iran, for providing financial support for this research. X-ray diffraction analyses were carried out at Gorgan University of Agricultural Sciences and Natural Resources. The authors acknowledge the constructive comments of Dr. Steven L. Forman, Baylor University, USA. The comments of the anonymous reviewers are highly appreciated.

References

Bajnóczi, B., Kovács-Kis, V., 2006. Origin of pedogenic needle-fiber calcite revealed by micromorphology and stable isotope composition – a case study of a Quaternary paleosol from Hungary. Geochemistry 66, 203–212.
Balsam, W.L., Ji, J., Chen, J., 2004. Climatic interpretation of the Luochuan and Lingtai loess section, China, based on changing iron oxide mineralogy. Earth and Planetary Science Letters 223, 335–348.
Balsam, W.L., Ellwood, B.B., Ji, J., Williams, R.R., Long, X., Hassani, A.E., 2011. Magnetic susceptibility as a proxy for rainfall: worldwide data from tropical and temperate climate. Quaternary Science Reviews 30, 2732–2744.
Barta, G., 2014. Paleoenvironmental reconstruction based on the morphology and distribution of secondary carbonates of the loess-paleosol sequence at Sütto, Hungary. Quaternary International 319, 64–75.
Barta, G., 2011. The structure and origin of loess dolls – a case study from the loess-paleosoil sequence of Sütto, Hungary. Journal of Environmental Geography 4 (1–4), 1–10.
Becze-Deák, J., Langohr, R., Verrecchia, E.P., 1997. Small scale secondary $CaCO_3$ accumulations in selected sections of the European loess belt. Morphological forms and potential for paleoenvironmental reconstruction. Geoderma 76, 221–252.
Begét, J.E., 2001. Continuous Late Quaternary proxy climate records from loess in Beringia. Quaternary Science Reviews 20, 499–507.
Begét, J.E., Hawkins, D.B., 1989. Influence of orbital parameters on Pleistocene loess deposition in central Alaska. Nature 337, 151–153.
Bronger, A., Bruhn-Lobin, N., Heinkele, T., 1994. Micromorphology of paleosols-genetic and paleoenvironmental deductions: case studies from central China, south India, NW Morocco and the Great Plains of the USA. In: Ringrose-Voase, A.J., Humphreys, G.S. (Eds.), Soil Micromorphology: Studies in Management and Genesis, Developments in Soil Science, vol. 22. Elsevier, Amsterdam, pp. 187–206.
Bullock, P., Federoff, N., Jongerius, A., Stoops, G., Tursina, T., Babel, U., 1985. Handbook for Soil Thin Section Description. Waine Research Publications, Wolverhampton (U.K).
Cailleau, G., Verrecchia, E.P., Braissant, O., Emmanuel, L., 2009. The biogenic origin of needle fibre calcite. Sedimentology 56, 1858–1875.
Catt, J.A., 1991. Soils as indicators of Quaternary climatic change in mid-latitude regions. Geoderma 51, 167–187.
Chen, J., Chen, L., Ji, J., Balsam, W., Sun, Y., Lu, H., 2006. Zr/Rb ratio in the Chinese loess sequences and its implication for changes in the East Asian winter monsoon strength. Geochimica et Cosmochimica Acta 70 (6), 1471–1482.
Chen, J., et al., 2015. Post-depositional forcing of magnetic susceptibility variations at Kurtak section, Siberia. Quaternary International. http://dx.doi.org/10.1016/j.quaint.2015.09.092.
Chen, Q., Liu, X.M., Heller, F., Hirt, A., Lü, B., Guo, X.L., Mao, X.G., Chen, J.S., Zhao, G.Y., Feng, H., Guo, H., 2012. Susceptibility variations of multiple origins of loess from the Ily Basin (NW China). Chinese Science Bulletin 57 (15), 1844–1855.
Chlachula, J., 2003. The Siberian loess record and its significance for reconstruction of pleistocene climate change in north-central Asia. Quaternary Science Reviews 22, 1879–1906.
Chlachula, J., Evans, M.E., Rutter, N.W., 1998. A magnetic investigation of a late Quaternary loess/palaeosol record in Siberia. Geophysical Journal International 132, 128–132.
Constantin, D., Begy, R., Vasiliniuc, S., Panaiotu, C., Necula, C., Codrea, V., Timar-Gabor, A., 2014. High-resolution OSL dating of the Costinesti section (Dobrogea, SE Romania) using fine and coarse quartz. Quaternary International 334–335, 20–29.
Cornell, R.M., Schwertmann, U., 2003. The Iron Oxides, second ed. John Wiley, New York, p. 664.
Dearing, J.A., Dann, R.J.L., Hay, K., Lees, J.A., Loveland, P.J., Maher, B.A., O'Grady, K., 1996. Frequency-dependent susceptibility measurements of environmental materials. Geophysical Journal International 124, 228–240.
Ding, Z.L., Ranov, V., Yang, S.L., Finaev, A., Han, J.M., Wang, G.A., 2002. The loess record in southern Tajikistan and correlation with Chinese loess. Earth and Planetary Science Letters 200 (3–4), 387–400.
Dodonov, A.E., 1991. Loess of Central Asia. GeoJournal 24, 185–194.
Dodonov, A.E., Baigusina, L.L., 1995. Loess stratigraphy of Central Asia: palaeoclimatic and palaeoenvironmental aspects. Quaternary Science Reviews 14, 707–720.
Dodonov, A.E., Gorshkov, A.I., Verkhovtseva, N.V., Sivtsov, A.V., Zhou, L.P., 2002. New data on the composition of magnetic minerals from paleosols of Southern Tajikistan. Lithology and Mineral Resources 37 (2), 186–193.
Dodonov, A.E., Zhou, L.P., Markova, A.K., Tchepalyga, A.L., Trubikhin, V.M., Aleksandrovski, A.L., Simakova, A.N., 2006. Middle–Upper Pleistocene bioclimatic and magnetic records of the Northern Black Sea Coastal Area. Quaternary International 159, 44–54.
Egli, M., Mirabella, A., Mancabelli, A., Sartori, A., 2004. Weathering of soils in alpine areas as influenced by climate and parent material. Clays and Clay Minerals 52, 287–303.
Evans, M.E., Rokosh, C.D., Rutter, N.W., 2002. Magnetoclimatology and paleoprecipitation: evidence from a north-south transect through the Chinese Loess Plateau. Geophysical Research Letters 29, 127-121–127-124.
Fang, X.M., Shi, Z.T., Yang, S.L., Yan, M.D., Li, J.J., Jiang, P.A., 2002. Loess in the Tian Shan and its implications for the development of the Gurbantunggut Desert and drying of northern Xinjiang. Chinese Science Bulletin 47 (16), 1381–1387.
Fedoroff, N., Courty, M.A., Guo, Z., 2010. Palaeosoils and relict soils. In: Stoops, G., Marcelino, V., Mees, F. (Eds.), Interpretation of Micromorphological Features of Soils and Regoliths. Elsevier, pp. 623–662.
Frechen, M., Kehl, M., Rolf, C., Sarvati, R., Skowronek, A., 2009. Loess chronology of the Caspian Lowland in Northern Iran. Quaternary International 128, 220–233.
Grimley, D.A., Arruda, N.K., 2007. Observations of magnetite dissolution in poorly drained soils. Soil Science 172 (12), 968–982.
Guo, Z., Biscaye, P., Wei, L., Chen, X., Peng, S., Liu, T., 2000. Summer monsoon variations over the last 1.2 Ma from the weathering of loess-soil sequences in China. Geophysical Research Letters 27, 1751–1754.
Heller, F., Tungsheng, L., 1984. Magnetism of Chinese loess deposits. Geophysical Journal International 77, 125–141.
Heller, F., Shen, C.D., Beer, J., Liu, X.M., Liu, T.S., Bronger, A., Suter, M., Bonani, G., 1993. Quantitative estimates of pedogenic ferromagnetic mineral formation in Chinese loess and palaeoclimatic implications. Earth and Planetary Science Letters 114, 385–390.
Hu, X.F., 2004. Influence of iron oxides and organic matter on magnetic susceptibility in the loess-paleosol sequence. Acta Pedologica Sinica 41 (1), 7–12.
Hu, X.F., Xu, L.F., Pan, Y., Shen, M.N., 2009a. Influence of the aging of Fe oxides on the decline of magnetic susceptibility of the Tertiary red clay in the Chinese Loess Plateau. Quaternary International 209, 22–30.
Hu, X.F., Wei, J., Xu, L.F., Zhang, G.L., Zhang, W.G., 2009b. Magnetic susceptibility of the Quaternary Red Clay in subtropical China and its paleoenvironmental implications. Palaeogeography, Palaeoclimatology, Palaeoecology 279, 216–232.
Hu, X.F., Cheng, T.F., Wu, H.X., 2003. Do multiple cycles of aeolian deposit-pedogenesis exist in the reticulate red clay sections in southern China. Chinese Science Bulletin 48 (12), 1251–1258.
Jackson, M.L., 1975. Soil Chemical Analysis, Advanced Course. University of Wisconsin, College of Agriculture, Department of Soil Science, Madison, WI.
Ji, J., Chen, J., Lu, H., 1999. Origin of illite in the loess from the Luochuan area, Loess Plateau, Central China. Clays and Clay Minerals 34, 525–532.
Ji, J., Chen, J., Xu, H., Chen, T., 2002. Chemical Weathering of Chlorite in Chinese Loess-paleosol Stratigraphy and Climate Change. Paper presented at Annual Meeting, Geol. Soc. of Am., Denver, Colo..
Jia, J., Liu, X.B., Xia, D.S., Wei, H.T., Wang, B., 2011. Magnetic property of loess strata recorded by Kansu profile in Tianshan Mountains. Journal of Arid Land 3 (3), 191–198.
Jia, J., Xia, D.S., Wang, B., Wei, H.T., Liu, X.B., 2012. Magnetic investigation of Late Quaternary loess deposition, Ili area, China. Quaternary International 250, 84–92.
Jiamao, H., Keppens, E., Tungsheng, L., Paepe, R., Wenying, J., 1997. Stable isotope composition of the carbonate concretion in loess and climate change. Quaternary International 37, 37–43.
Johns, W.D., Grim, R.E., Bradley, W.F., 1954. Quantitative estimation of clay minerals by diffraction methods. Journal of Sedimentary Petrology 24, 242–251.
Karimi, A., Frechen, M., Khademi, H., Kehl, M., Jalalian, A., 2011. Chronostratigraphy of loess deposits in northeast Iran. Quaternary International 234, 124–132.
Karimi, A., Khademi, H., Kehl, M., Jalalian, A., 2009. Distribution, lithology and provenance of peridesert loess deposits in northeastern Iran. Geoderma 148, 241–250.
Kehl, M., Sarvati, R., Ahmadi, H., Frechen, M., Skowronek, A., 2005. Loess paleosol-sequences along a climatic gradient in Northern Iran. Quaternary Science Journal 55, 151–175.
Kehl, M., 2010. Quaternary loesses, loess-like sediments, soils and climate change in Iran. In: Relief, Boden, Palaoklima, vol. 24, p. 208.
Kehl, M., 2009. Quaternary climate change in Iran. The state of knowledge. Erdkunde 63 (1), 1–17.
Kemp, R.A., 1998. Role of micromorphology in paleopedological research. Quaternary International 51/52, 133–141.
Khormali, F., Kehl, M., 2011. Micromorphology and development of loess-derived surface and buried soils along a precipitation gradient in Northern Iran. Quaternary International 234, 109–123.
Khormali, F., Abtahi, A., Mahmoodi, S., Stoops, G., 2003. Argillic horizon development in calcareous soils of arid and semiarid regions of southern Iran. Catena 53, 273–301.
Khormali, F., Abtahi, A., 2003. Origin and distribution of clay minerals in calcareous arid and semi-arid soils of Fars Province, southern Iran. Clay Minerals 38, 511–527.
Khormali, F., Abtahi, A., Stoops, G., 2006. Micromorphology of calcitic features in highly calcareous soils of Fars Province, Southern Iran. Geoderma 132, 31–46.

Kittrick, J.A., Hope, E.W., 1963. A procedure for particle size separation of soils for X-ray diffraction analysis. Soil Science 96, 312–325.
Kravchinsky, V.A., Zykina, V.S., Zykin, V.S., 2008. Magnetic indicator of global paleoclimate cycles in Siberian loess-paleosol sequences. Earth and Planetary Science Letters 265, 498–514.
Kukla, G., An, Z., 1989. Loess stratigraphy in Central China. Palaeogeography, Palaeoclimatology, Palaeoecology 72, 203–225.
Lauer, T., et al., 2015. Luminescence-chronology of the loess palaeosol sequence Toshan, Northern Iran – a highly resolved climate archive for the last glacial–interglacial cycle. Quaternary International. http://dx.doi.org/10.1016/j.quaint.2015.03.045.
Liu, Q., Deng, C., Yu, Y., Torrent, J., Jackson, M.J., Banerjee, S.K., Zhu, R., 2005. Temperature dependence of magnetic susceptibility in an argon environment: implications for pedogenesis of Chinese loess/palaeosols. Geophysical Journal International 161, 102–112.
Liu, T.S., Ding, Z.L., 1998. Chinese loess and the paleomonsoon. Annual Review of Earth and Planetary Sciences 26, 111–145.
Liu, T.S., et al., 1985. Loess and the Environment. China Ocean Press, Beijing (unnamed).
Liu, X., Liu, T., Paul, H., Xia, D., Jiri, C., Wang, G., 2008. Two pedogenic models for paleoclimatic records of magnetic susceptibility from Chinese and Siberian loess. Science in China Series D: Earth Sciences 51, 284–293.
Liu, X.M., Xia, D., Liu, D.S., 2007. Discussion on two models of paleoclimatic records of magnetic susceptibility of Alaskan and Chinese loess (in Chinese). Quaternary Sciences 27, 210–220.
Liu, X.M., Liu, T.S., Heller, F., Xu, T.C., 1990. Frequency dependent susceptibility of loess and Quaternary paleoclimate. Quaternary Sciences 1, 41–50.
Liu, X.M., Shaw, J., Heller, F., 1992. Magnetic mineralogy of Chinese loess and its significance. Geophysical Journal International 108, 301–308.
Liu, X.M., Liu, Z., Lü, B., Markovic, S.B., Chen, J.S., Guo, H., Ma, M.M., Zhao, G.Y., Feng, H., 2012. The magnetic properties of Serbian loess and its environmental significance. Chinese Science Bulletin 58, 353–363.
Liu, X.M., Hesse, P., Rolph, T., Beget, J.E., 1999. Properties of magnetic mineralogy of Alaskan loess: evidence for pedogenesis. Quaternary International 62, 93–102.
Liu, X.M., Hesse, P., Beget, J., Rolph, T., 2001. Pedogenic destruction of ferrimagnetics in Alaskan loess deposits. Soil Research 39, 99–115.
Liu, X.M., Rolph, T., An, Z.S., Hesse, P., 2003. Paleoclimatic significance of magnetic properties on the red clay underlying the loess and paleosols in China. Palaeogeography, Palaeoclimatology, Palaeoecology 199, 153–166.
Machalett, B., Oches, E.A., Frechen, M., Zoller, L., Hambach, U., Mavlyanova, N.G., Markovic, S., Endlicher, W., 2008. Aeolian dust dynamics in central Asia during the Pleistocene: driven by the long-term migration, seasonality, and permanency of the Asiatic polar front. Geochemistry Geophysics Geosystems 9 (8), 1–22.
Maher, B.A., 1998. Magnetic properties of modern soils and Quaternary loessic paleosol: paleoclimatic implication. Palaeogeography, Palaeoclimatology, Palaeoecology 137, 25–54.
Maher, B.A., Thompson, R., Zhou, L.P., 1994. Spatial and temporal reconstructions of changes in the Asian palaeomonsoon: a new mineral magnetic approach. Earth and Planetary Science Letters 125, 461–471.
Maher, B.A., Thompson, R., 1995. Paleorainfall reconstructions from pedogenic magnetic susceptibility variations in the Chinese loess and paleosols. Quaternary Research 44, 383–391.
Mehra, O.P., Jackson, M.L., 1960. Iron oxide removal from soils and clays by a dithionite-citrate system buffered with sodium bicarbonate. Clays and Clay Minerals 5, 317–327.
Meier, H.A., Driese, S.G., Nordt, L.C., Forman, S.L., Dworkin, S.L., 2014. Interpretation of Late Quaternary climate and landscape variability based upon buried soil macro- and micromorphology, geochemistry, and stable isotopes of soil organic matter, Owl Creek, central Texas, USA. Catena 114, 157–168.
Meng, X., Derbyshire, E., Kemp, R.A., 1997. Origin of the magnetic susceptibility signal in Chinese loess. Quaternary Science Reviews 16, 833–839.
Muhs, D.R., 2007. Loess deposits, origins and properties. In: Elias, S.A. (Ed.), Encyclopedia of Quaternary Science. Elsevier, Oxford.
Murphy, C.P., 1986. Thin Section Preparation of Soils and Sediments. A B Academic Publishers, Berhamsted, UK.
Reheis, M.C., 1987. Climatic implications of alternating clay and carbonate formation in semiarid soils of South-Central Montana. Quaternary Research 27, 270–282.
Salinity Laboratory Staff, 1954. Diagnosis and Improvement of Saline and Alkali Soils. United States Department of Agriculture Handbook No. 60 Washington, DC.
Shi, Z.T., 2005. The Age of Loess Sediments in Yili Area of Xinjiang and Its Paleoenvironment Significances. Postdoctoral Report. Institute of Earth Environment, Chinese Academy of Sciences, Xi'an, pp. 1–125 (in Chinese, with English Abstract).
Soil Survey Staff, 2014. Keys to Soil Taxonomy. U.S. Department of Agriculture, Natural Resources Conservation Service.
Song, Y.G., Shi, Z.T., Fang, X.M., Nie, J.S., Naoto, I., Qiang, X.K., Wang, X.L., 2010a. Loess magnetic properties in the Ili Basin and their correlation with the Chinese Loess Plateau. Science in China: Earth Sciences 53 (3), 419–431.
Song, Y., et al., 2013. Magnetic parameter variations in the Chaona loess/paleosol sequences in the central Chinese Loess Plateau, and their significance for the middle Pleistocene. Quaternary Research 81 (3), 433–444.
Song, Y.G., Shi, Z.T., Dong, H.M., Nie, J.S., Qian, L.B., Chang, H., Qiang, X.K., 2008. Loess magnetic susceptibility in Central Asia and its paleoclimatic significance. In: International Geoscience and Remote Sensing Symposium, vol. 2, pp. 1227–1230.
Song, Y.G., Nie, J.S., Shi, Z.T., Wang, X.L., Qiang, X.K., Chang, H., 2010b. A preliminary study of magnetic enhancement mechanisms of the Tianshan loess. Journal of Earth Environment 1 (1), 60–67.
Stoops, G., 2003. Guidelines for the Analysis and Description of Soil and Regolith Thin Sections. Soil Science Society of America, Madison, WI.
Stoops, G., Marcelino, V., Mees, F., 2010. Interpretation of Micromorphological Features of Soils and Regoliths, first ed. Elsevier Science, p. 752.
Sun, J., Liu, T., 2000. Multiple origins and interpretations of the magnetic susceptibility signal in Chinese wind-blown sediments. Earth and Planetary Science Letters 180, 287–296.
Verrecchia, E.P., Verrecchia, K.E., 1994. Needle-fiber calcite: a critical review and a proposed classification. Journal of Sedimentary Research 64 (3), 650–664.
Vlaminck, S., et al., 2015. Loess-soil sequence at Toshan (Northern Iran): insights into late Pleistocene climate change. Quaternary International. http://dx.doi.org/10.1016/j.quaint.2015.04.028.
Wang, X., et al., 2016. Grain-size distribution of Pleistocene loess deposits in northern Iran and its palaeoclimatic implications. Quaternary International. http://dx.doi.org/10.1016/j.quaint.2016.01.058.
Wang, X., Lu, H., Li, Z., Deng, C., Tan, H., Song, Y.G., 2003. Peloclimatic significance of mineral magnetic properties of loess sediments in northeastern Qinghai-Tibetan Plateau. Chinese Science Bulletin 48, 2126–2133.
Wilding, L.P., Drees, L.R., 1988. Removal of carbonate from thin sections for microfabric interpretations. In: Fedoroff, N., Bresson, L.M., Courty, M.A. (Eds.), Soil Micromorphology, Proceedings of the 7th International Working Meeting on Soil Micromorphology. AFES, Paris, pp. 653–665.
Yang, S., Forman, S.L., Song, Y., Pierson, J., Mazzocco, J., Li, X., Shi, Z., Fang, X., 2014. Evaluating OSL-SAR protocols for dating quartz grains from the loess in Ili Basin, Central Asia. Quaternary Geochronology 20, 78–88.
Yang, S., Ding, F., Ding, Z., 2006. Pleistocene chemical weathering history of Asian arid and semi-arid regions recorded in loess deposits of China and Tajikistan. Geochimica et Cosmochimica Acta 70, 1695–1709.
Zhao, L., Ji, J.F., Chen, J., Liu, L.W., Chen, Y., Balsam, W., 2005. Variations of illite/chlorite ratio in Chinese loess sections during the last glacial and interglacial cycle: implications for monsoon reconstruction. Geophysical Research Letters 32, L20718. http://dx.doi.org/10.1029/2005GL024145.
Zhou, L.P., Oldfield, F., Wintle, A.G., Robinson, S.G., Wang, J.T., 1990. Partly pedogenic origin of magnetic variations in Chinese loess. Nature 346, 737–739.
Zhu, R., Alexey, K., Galina, M., Guo, B., Zykina, V., Eduard, P., Neli, J., 2000. Rock-magnetic investigation of Siberia loess and its implication. Chinese Science Bulletin 45, 2192–2198.
Zhu, R., Matasova, G., Kazansky, A., Zykina, V., Sun, J., 2003. Rock magnetic record of the last glacial-interglacial cycle from the Kurtak loess section, southern Siberia. Geophysical Journal International 152, 335–343.

https://doi.org/10.1016/j.yqres.2016.05.004 Published online by Cambridge University Press